



ISSN: 0067-2904

## Eco-Friendly synthesis of Nickel oxide Nanoparticles Using Licorice leaves extract for anticancer effect against bone cancer cells MG-63 and Antibacterial Activity

Mohammed mahmood masood\* ,Wadhah Naji Jassim Al Sieadi  
Department of Chemistry, College of Science, University of Baghdad, Baghdad, Iraq

Received: 18/5/2024 Accepted: 10/9/2024 Published: 30/9/2025

### Abstract

In this study, nickel oxide nanoparticles (NiO-NPs) were synthesized using nickel nitrate hexahydrate and licorice leaves extract, which served as both a reducing agent and a capping agent. The optical, structural, and microscopic properties of the NiO-NPs were characterized using a range of techniques, including UV-visible spectroscopy, Fourier transform infrared spectroscopy, energy-dispersive X-ray analysis, field emission scanning electron microscopy, and atomic force microscopy. The bio-reducing potential of Licorice leaves was examined using gas chromatography-mass spectroscopy for phytochemical analysis of plant extract. Furthermore, cell cytotoxicity investigation was conducted on the Mg-63 cell line derived from osteosarcoma by the MTT method. The results showed that the viability of cancer cells was reduced with increasing NiO NPs concentration up to 28.78% for MG-63 Cells at the maximum concentration (500 µg/ml) in comparison with 80.79 % for HFF cell viability as control cells, while the antimicrobial experiments have demonstrated that NiO-NP action of two types of gram-positive bacteria and for two types of gram-negative bacteria. The results showed that NiO NPs had the highest antibacterial activity at high concentrations (1024 ug/ mL), forming the largest inhibition zone against Escherichia coli, Pseudomonas aeruginosa, Staphylococci aureus and Streptococcus with inhibition zones 18mm,18mm ,15mm and 22 mm respectively.

**Keywords:** Nickel oxide nanoparticles, Licorice leaves, Anticancer, MG-63, Antibacterial

التخليق الصديق للبيئة لأكاسيد النيكل النانوية باستخدام مستخلص أوراق عرق السوس لبيان فعاليتها  
المضادة للسرطان ضد خلايا سرطان العظام MG-63 ولنشاطها المضادة للبكتيريا

محمد محمود مسعود\* , وضاح ناجي جاسم السعدي

قسم الكيمياء , كلية العلوم , جامعة بغداد , العراق

### الخلاصة

تم تصنيع جسيمات أكسيد النيكل النانوية (NiO-NPs) باستخدام نترات النيكل ومستخلص أوراق عرق السوس التي تعمل على اختزال جسيمات النيكل وتغطيتها. وتحديد الخصائص البصرية والبنية والمجهرية

\*Email: [Mohammed.mahmoud1105d@sc.uobaghdad.edu.iq](mailto:Mohammed.mahmoud1105d@sc.uobaghdad.edu.iq)

لجسيمات أكسيد النيكل النانوية باستعمال مجموعة من التقنيات، منها التحليل الطيفي للأشعة فوق البنفسجية والمرئية، والتحليل الطيفي للأشعة تحت الحمراء، وتحليل الأشعة السينية المشتتة للطاقة، والمجهر الإلكتروني الماسح، ومجهر القوى الذرية.

تم تشخيص المكونات الحيوية لمستخلص أوراق عرق السوس باستعمال تقنية كروماتوغرافيا الغاز-مطيافية الكتلة. علاوة على ذلك فقد تمت دراسة سمية المواد على الخلايا في المختبر على خط خلية Mg-63 المشتق من ساركوما العظام بطريقة MTT.

أظهرت النتائج أن قابلية خلايا السرطان للبقاء على قيد الحياة انخفضت مع زيادة تركيز جسيمات البكتيريا إيجابية الجرام حتى 28.78% لخلايا MG-63 عند أقصى تركيز (500 ميكروغرام / مل) بالمقارنة مع 80.79% لقدرة خلايا HFF على البقاء على قيد الحياة بوصفها خلايا تحكم، في حين أثبتت التجارب المضادة للميكروبات أن تأثير جسيمات أكسيد النيكل النانوية على نوعين من البكتيريا إيجابية الجرام ونوعين من البكتيريا سلبية الجرام، وأظهرت الأنواع المختلفة مستويات متفاوتة من القابلية للتأثر، مع أعلى منطقة تثبيط في تركيزات عالية من جسيمات أكسيد النيكل النانوية (1024 ميكروغرام / مل) ضد الإشريكية القولونية والزائفة الزنجارية والمكورات العنقودية الذهبية والعقدية مع مناطق تثبيط 18 مم و15 مم و22 مم على التوالي.

## 1. Introduction

Osteosarcoma (OS) is a rare and heterogeneous tumor that originates from mesenchymal cells, characterized by a significant diversity of subtypes. Osteosarcoma primarily affects children and adolescents, with the highest incidence observed in two age groups: those 18 years old and 60 years old. Males are more commonly impacted than girls. Approximately 80% of instances involving the Osteosarcoma impact the limbs, namely the long bones. This can be linked to the fast development and bone turnover throughout adolescence. The remaining instances primarily occur in the axial skeleton, with occasional occurrences in the jaw or hand [1]. The global occurrence of this condition is estimated to be around 1-5 instances per million individuals annually. Between 10% and 15% of cases of this condition may be attributed to a specific cause, while the rest of the cases have an unknown explanation [2]. Several potential risk factors have been identified, including bone infarct, osteochondroma, Paget's disease, and previous irradiation. The high rate of bone growth that takes place throughout adolescence, particularly at the metaphysis of lengthy bones, may clarify the connection between the common incidence of osteosarcoma at these locations and developmental phases [3].

The integration of nanotechnology with biology facilitates the development of more efficient anticancer and antimicrobial agents for promising solutions to overcome the proliferation of cancer cells and enhance the targeted drug delivery with the least effect on normal cells [4-7].

The green synthesis of nanoparticles utilizes plant extracts as reducing and capping agents, thereby reducing the use of toxic chemicals [8]. Plant extracts contain various phytochemical compounds such as flavonoids, terpenoids, alkaloids, sugars, and proteins, which convert metal ions into metal atoms to form nanoparticles. However, the structure, size and morphological nature of nanoparticles depend on the bioactive phytochemicals current in the plant extract [9, 10].

In recent years, NiONPs have been synthesized using environmentally friendly techniques and have garnered significant praise for their simplicity, cost-effectiveness, photo-stable, and abundantly availability. Their biological applications which includes antioxidant and antimicrobial activities that can have significant impact in various biomedical fields [11, 12].

Licorice originates from the stem and root parts of *Glycyrrhiza glabra* (*G. glabra*), a small perennial plant native to the Mediterranean region, central and southwest Asia. *G. glabra* is the botanical source of licorice. In China, licorice goes by the name "gan cao", being derived from the underground portions of *G. glabra* grown in those areas. The ancient Greek physician Pedanius Dioscorides used the term (*glukurrhiza*) refer to licorice, meaning "sweet root". Egyptian pharaohs were commonly utilized as a flavoring agent [13].



**Figure 1:** Licorice plant

*Glycyrrhiza glabra* is a plant that can reach a height of 2.5 meters. The leaves are compound, composed of 4-7 pairs of oblong, elliptical or lanceolate leaflets. The flowers are delicate and may exhibit a typical pea-like, papilionaceous structure. They are arranged in axillary spikes and exhibit pale lavender to violet coloration. The fruit is a condenser legume or pod, up to 1.5cm long and usually contains 3-5 brown reniform seeds. The taproot is around 1.5cm long and split into 3-5 secondary roots [14].

They are used in plant-based medications, health products, pharmaceuticals and dietary supplements. Licorice is also a common and useful ingredient in Tobacco products and cosmetics [15].

Numerous studies have highlighted the benefit of licorice root and its bioactive constituents including carbenoxolone, glycyrrhizic acid, dehydroglyasperin C, 18 $\beta$ - dehydroglyasperin D and glycyrrhetic acid, in addition to unique materials like licochalcone, licoricidin, licorisoflavan and glabridin, these materials may have a positive effect on human healthy [16].

Licorice is regarded as a natural medicine for several diseases such as tuberculosis, wound healing, cough, and diabetes [17]. In Traditional Chinese medicine (TCM), licorice is one of the widely used herbs [18]. These effects have been linked with anti-inflammatory, Antiulcer activity [19], Immunostimulatory activity, Anti-fungal activity, Anti-malarial activity [20], Antioxidant activity [21], Anti-tussive, Anti-bacterial Activity [22]. Anti-viral effects [23], Antithrombotic effect, Hair growth stimulation and Skin lightening activity [24].

The aerial parts of the plant are rarely utilized and are often regarded as waste products. However, recent investigations have focused on the aerial parts of plants (leaves) belonging to investigate their antioxidant, anti-genotoxic and anti-inflammatory activities [25, 26].

O. Chouitah, B. Meddah, A. Aoues, and P. Sonnet investigated the chemical composition and antimicrobial activities of the essential oil from *glycyrrhiza glabra* Leaves by hydrodistillation and analyzed by GC and GC-MS [27]. While D. M. Biondi, C. Rocco, and

G. Ruberto studied the New dihydrostilbene derivatives from the Leaves of *Glycyrrhiza glabra* and evaluation of their antioxidant activity [28].

Y.dong, M.Zhao, D. Sun Waterhouse, M.Zhuang, H. Chen, M. Feng and L.Lin. investigated the adsorption and desorption properties of flavonoids extracted from *Glycyrrhiza glabra* L. leaves using macroporous resins in a study published in [29]. In addition, the productive use of agrochemical wastes currently seems to enhance the accessibility at bioactive natural compounds And demonstrate the extent of its benefit in various medical and environmental fields [30].

The present study aims to determine the biological activity of green fabricated nickel oxide nanoparticles from Nickel nitrate hexahydrate and Licorice leaves as anticancer agents and antibacterial activity.

## 2. Materials and Methods

### 2.1. Materials

The leaves of licorice (*Glycyrrhiza glabra* L.) were collected from a village in Diyala government, Iraq in May 2023. Nickel nitrate hexahydrate (99% purity, BHD, Germany), sodium hydroxide (97% purity Sigma-Aldrich, USA). Agar, nutrient, ethanol, and Dimethyl sulfoxide (DMSO) (99% purity) were supplied from Sigma-Aldrich. Fetal bovine serum (FBS) (Welgene, a company, South Korea). 3-(4,5-dimethylthiazol-2-yl)-2,5-diphenyl tetrazolium bromide (MTT) was supplied from Sigma, USA.

### 2.2. Instrumentation

The characterization of the synthesised nanoparticles was conducted using Scanning Electron Microscope (SEM, MIRA3, USA), X-Ray Diffraction (XRD, XD-3, persee, China), Fourier-transform infrared (FTIR, SHIMADZU 8400S, Japan), Atomic Force Microscopy (AFM, Nanosurf AG, Switzerland), and UV-visible spectroscopy (UV-VIs. SHEMADZU 260, Japan). The GC-MS analysis was performed using GCMS-QP2010 PLUS apparatus. MTT Assay was measured at a wavelength of 570 nm using an Elisa plate reader (Model 50, Bio-Rad Corp, Hercules, California, CA).

### 2.3. Aqueous Extraction *Licorice* leaves

Licorice (*Glycyrrhiza glabra* L.) leaves were carefully detached from the stems. To remove any dust, the leaves underwent multiple rinses with distilled water. They were then left to dry for a week. After drying, the leaves were ground into a fine powder using an electric grinder. The resulting powder was stored in a glass container and kept at room temperature. A mass of 5 grams of finely ground powder was added to 100 mL of distilled water. This mixture was then heated to 70 degrees Celsius and maintained at that temperature for a duration of 30 minutes. Once cooled, the extracted solution underwent filtration using Whatman filter paper to remove impurities. The resulting filtrate was then collected and stored at 4 C to be saved for future testing or use [31].

### 2.4. Synthesis of nickel Oxide Nanoparticles from *Licorice* leaves

The green synthesis of NiO NPs was performed using an extract from licorice leaves. 14.54 gms of Nickel (II) nitrate solution was dissolved in 50 mL of deionized water to prepare the stock solution of 1 M as Nickel precursor salt and stirred for 10 min. Then, 12.5 mL aqueous extraction of *Licorice* leaves was added drop by drop and stirred for 30 min with a volumetric mixing ratio of 4 parts solvent to 1 part solute. A color change was detected initially, suggesting the formation of NiO-NPs. Then solution 1 M of NaOH was added slowly, and the pH of the mixture was precisely adjusted to 10 with continuously stirred under heating to

70°C for two hours. Upon completion of the reaction, verification was attained when the mixture exhibited a light green color [32]. Subsequently, the precipitates were gathered via collection and rinsed multiple times with distilled water. Next, the washed precipitates were left to air dry. To complete the synthesis, the dried sample was then calcined at 400 degrees Celsius for a period of two hours. This final calcination step yielded a black powder composed of nickel oxide (NiO) nanoparticles, as shown in Figure 2.

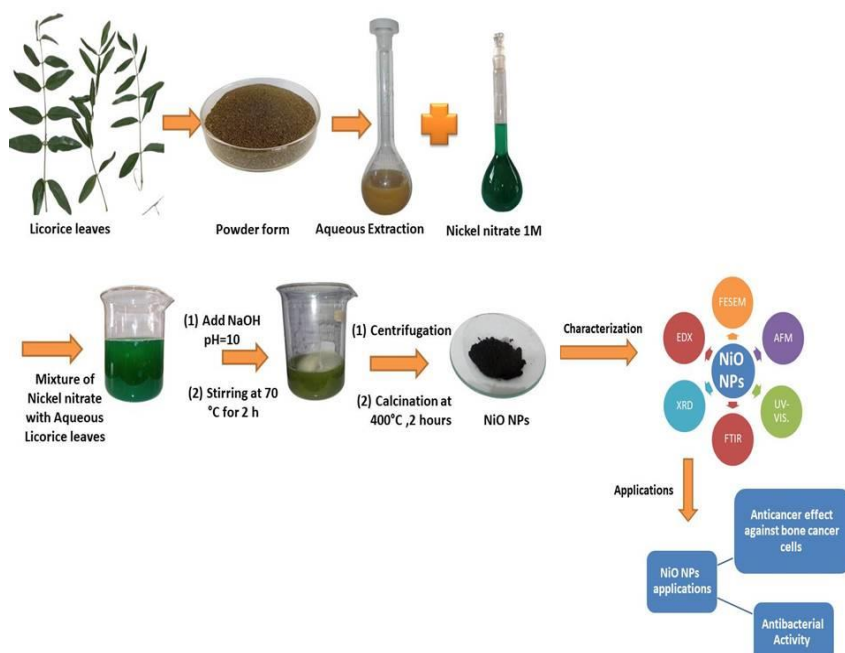


**Figure. 2:** Schematic illustrating the green synthesized of NiO NPs from Licorice leaves.

## 2.5. Antibacterial test for nickel oxide nanoparticles

The well-diffusion method was employed to examine the sensitivity of NiO NPs. This was accomplished by measuring the antimicrobial efficacy which was evaluated against two species each of Gram-negative bacteria (*Pseudomonas aeruginosa* and *Escherichia coli*) and Gram-positive bacteria (*Staphylococcus aureus* and *Streptococcus*), which were swabbed on nutrient agar at 37 °C for 24 hrs.

Wells with a diameter of 5 mm were created in the pre-existing agar layer, with four wells per plate. The agar discs were then removed, and a stock solution was prepared by dissolving 50 mg of green-fabricated NiO nanoparticles in 1 mL of Dimethyl sulfoxide (DMSO). 50 µl of NiO NPs for a set of four concentrations (128, 256, 512 and 1024 µg/mL) were added to each well using a micropipette and the DMSO solvent was added to the middle well as a control. The culture plates were incubated at 37 °C for 24 hrs. and the results of the inhibition zone were recorded [11, 33].

## 2.6. Cytotoxicity test of NiO NPs

The cytotoxic property of the green synthesized NiO NPs derived from Licorice leaves was carried out against the human osteosarcoma cell line (MG 63) by using an MTT assay. The cells were cultured and the cell suspension was diluted with a solution containing 5% fetal bovine serum (FBS) to achieve a final density of  $1 \times 10^5$  cells/ml. The cell line was then seeded into 96-well titer plates and incubated to allow for cell adhesion at 37 °C, 5% CO<sub>2</sub>, 95% air and 100% relative humidity. Then the plate was filled with various number of doses



(20-500  $\mu\text{g/ml}$ ) of synthesized NiO NPs by dispersed particles in cell culture media and subjected to sonication for 10 minutes to create a stock solution with a concentration of 2 mg/mL. Subsequently, 150  $\mu\text{l}$  of nanoparticles dispersion were added to each well and the plates were incubated for an additional 24 hours at 37  $^{\circ}\text{C}$ . After the 24 h incubation 25  $\mu\text{L}$  of MTT (3-[4,5-dimethylthiazol-2-yl]2,5-diphenyltetrazolium bromide) (5 mg/mL) in phosphate- buffered saline (PBS) was added to each well and incubated at 37  $^{\circ}\text{C}$  for 4 hours. The tetrazolium salt is employed for evaluating cell viability in assays of cell growth and cytotoxicity. After removing the MTT medium, the formazan crystals were dissolved in 100 $\mu\text{l}$  of DMSO. Following dissolution, the absorbance of the solution was measured at 570 nm using a microplate reader. The cell inhibition percentage was then calculated using Equation 1[34]:

$$\text{Viability Percentage} = \frac{(\text{OD sample} - \text{OD blank})}{(\text{OD control} - \text{OD blank})} * 100 \quad (1)$$

where OD<sub>sample</sub>, OD<sub>control</sub> are the optical density values for experimental cells and control cells, respectively. OD<sub>blank</sub> is the absorbance of the cell counting kit solution.

### 3. Results and Discussion

#### 3.1. Characterization of NiO NPs.

##### 3.1.1. UV-Visible Analysis of NiO NPs.

Absorption spectra and optical energy gap were calculated using a UV–visible spectrophotometer. The UV-Vis absorption spectra of the biosynthesized NiO nanoparticles and aqueous extract of licorice leaves are presented in Figure 3A. The NiO nanoparticles exhibited a peak plasmon resonance centered around 295 nm, characteristic of their surface plasmon absorption. The energy band gap (Eg) was determined using Tauc's equation as shown in Eq. (2).

$$\alpha h\nu = P(h\nu - E_g)^x \quad (2)$$

Where  $\alpha$  is the coefficient of absorption,  $h\nu$  mean an incident photon energy, P is a constant and  $x$  rules the direct transition. The band gap value is equal to 3.69 eV which obtained by drawing the  $(\alpha h\nu)^2$  axis against energy by including the linear part of the graph as shown in Figure (3-B). As particle size decreases due to confinement in one dimension, the movement of particles is restricted, leading to an increase in energy band spacing through the phenomenon known as quantum confinement [35-37].

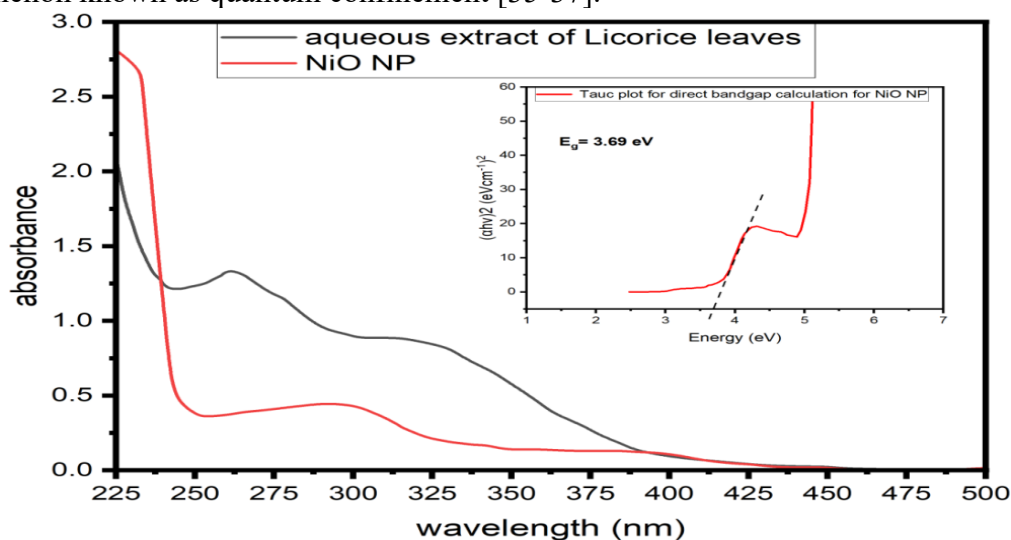


**Figure 3: (A)** UV-Visble absorbance spectra, and **(B)** the Tauc plot for direct bandgap of green synthesized NiO NPs using *Licorice* leaves extract.

### 3.1.2. FTIR Chemical Analysis

FTIR spectroscopy was employed to determine the functional groups responsible for the capping, reduction, and stabilization of the biosynthesized Nickel Oxide nanoparticles (NiONPs). Figure 4 demonstrates that the FTIR analysis of the aqueous Licorice leaves extract and NiONPs between 4000 to 400  $\text{cm}^{-1}$  range. The FTIR spectra of NiONPs showed the existence of multiple absorption peaks at 3479.58, 1649.14, 1541.12, 1456.26, 1382.96, and 1043.49, 927.76, 829.39 and 416.62  $\text{cm}^{-1}$ . During treatment of  $\text{Ni}(\text{NO}_3)_2 \cdot 6\text{H}_2\text{O}$  solution with Licorice leaves extract, the FTIR spectrum showed a change in its absorption peaks, which detected the reduction in Ni(II) and also acted as a capping and stabilizing agent for the synthesized nanoparticle. The presence of a notable characteristic peak at 416.62  $\text{cm}^{-1}$  due to the presence of Ni–O bond vibration indicated the creation of the metal–oxide (Ni=O) bond, which validated the configuration of NiO NPs. The broad absorption peak which observed at 3479.58  $\text{cm}^{-1}$  corresponds to the O–H stretching of the free hydroxyl group, it can be attributed to the polyphenolic constituents of the Licorice leaves extract. The absorption peak observed at 1649.14  $\text{cm}^{-1}$  indicated the presence of the C=O stretching in carboxylic acids or aromatic compounds while the peak at 1541.12 for C=C stretching of alkenes while a peak at 1456.26, 1382.96 and 1043.49  $\text{cm}^{-1}$  demonstrated the presence of O–H bending for carboxylic acid, alcohol, and C–O stretching (tertiary alcohol or aliphatic ether) respectively while the small bands observed at 927.76 and 829.39  $\text{cm}^{-1}$  correspond metal–oxygen stretching vibrations. and it was confirmed by the previous works[38 ,33].

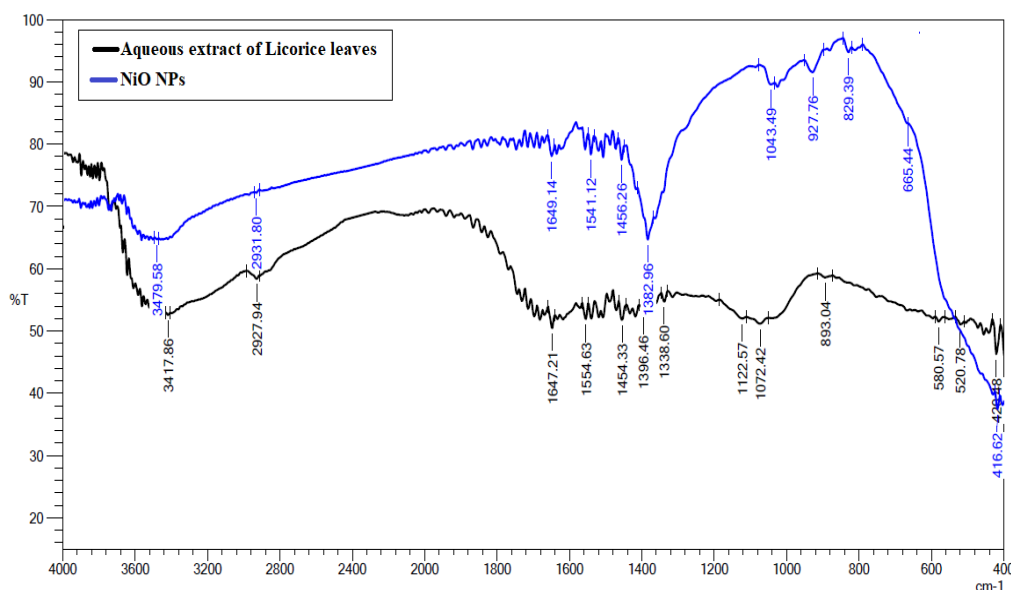


**Figure 4:** FTIR spectra for the aqueous extraction of *Licorice* leaves and NiO nanoparticles

### 3.1.3. X-ray Diffraction (XRD)

The XRD technique was employed to analyse phase purity and crystalline state of NiO and indicated the presence of five diffraction peaks with  $2\theta$  values of 37.350°, 43.380°, 62.980°, 75.410°, and 79.460° corresponding to the crystal planes of (003), (012), (110), (021), and (006) respectively as shown in Figure (5). These peaks were found to be in good agreement with the standard JCPDS data card number (00-022-1189). The XRD pattern exhibited distinct diffraction peaks, each characteristic of the rhombohedral crystal structure of the synthesized NiO [10].

The mean size of NiO NPs was determined to be 22.82 nm which was determined by Scherrer's formula which involves the Full-width half maxima and peak position of an XRD pattern as shown in Eq. (3).

$$D = k\lambda/\beta \cos \theta \quad (3)$$

where "D" is the crystallite size (nm), "k" is Scherrer's constant, equal to 0.98 and "θ" is the angle of diffraction. As shown in table (1)

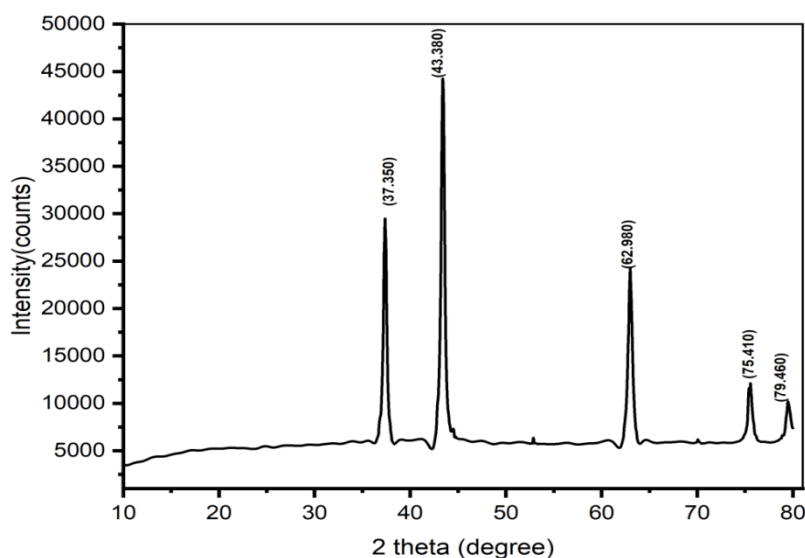


**Figure 5:** XRD patterns of NiO nanoparticles

**Table 1:** X-ray diffraction information for NiO NPs and average particle size calculated by Scherer equation

Pos.[°2Th.]	FWHM Left[°2Th.]	d-spacing [Å°]	Crystallite size (nm) D	Average Crystallite size (nm)
37.35	0.422	2.4056	20.3	22.82
43.38	0.438	2.0842	19.9	
62.98	0.498	1.4746	19.0	
75.41	0.378	1.2595	27.1	
79.46	0.379	1.2051	27.8	

### 3.1.4. Morphology and Elemental analysis

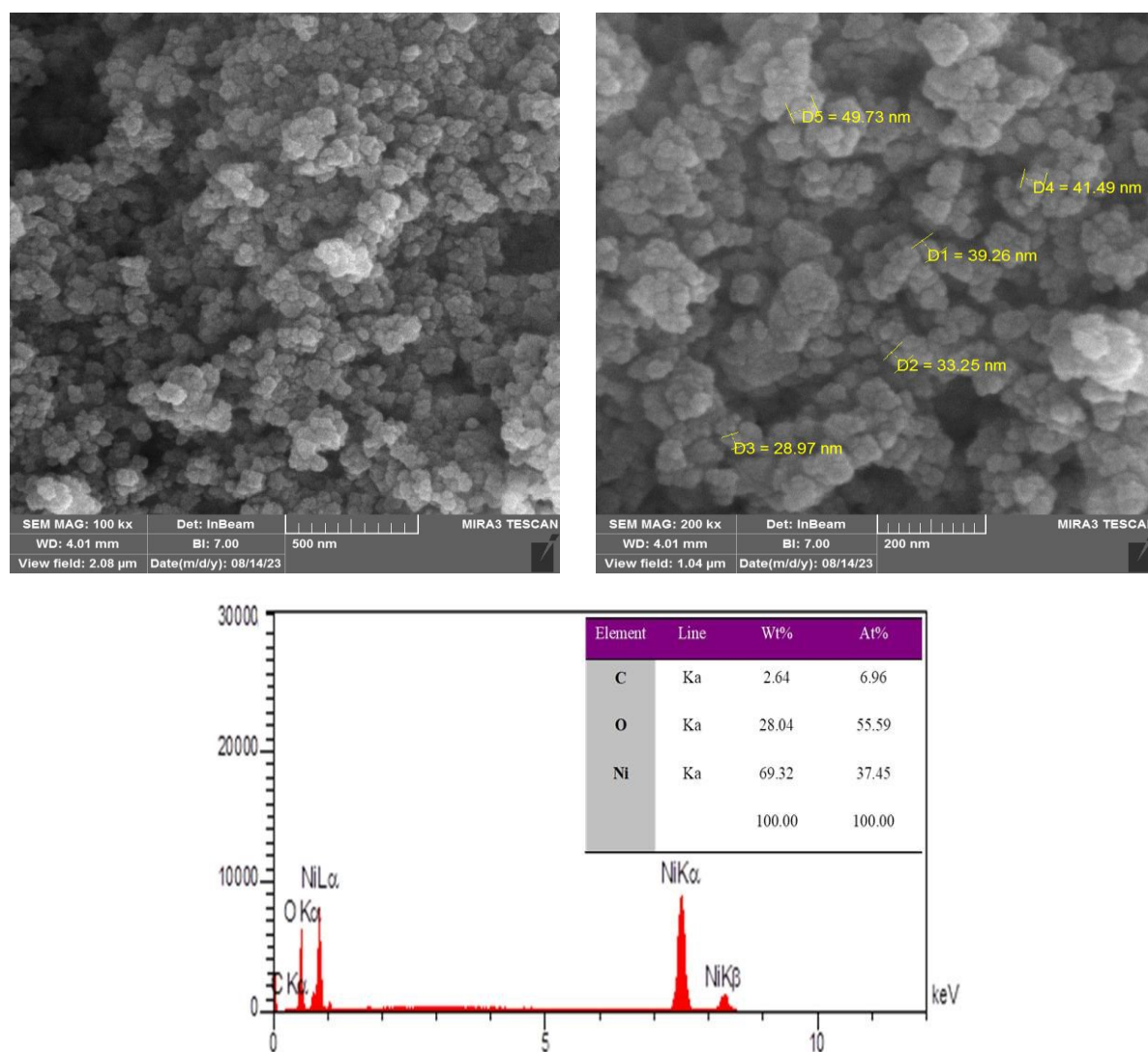
A scanning electron microscope (SEM) was utilized to examine the surface morphological characteristics of produced NiO nanoparticles .

Figure (6-A) shows The SEM images of the NiO powder annealed at 400°C. From the figure, it can be observed that the particles have a spherical shape with particle size between (28.97-49.73 nm) with some agglomerations, which may be attributed to hydrogen bond and electrostatic interactions of the bio-organic capping molecules bond of plant extract .[39]

The presence of pure NiO nanoparticles was also verified by energy-dispersive X-ray spectroscopy (EDS). Figure (6-B) display the elemental composition of NiO nanoparticles with significant signals for Ni(37.45%), confirming the synthesis of NiO NPs, in addition to a minor proportion of carbon(6.96 %) components attributed to the varying abundance and composition of capping agents of the extract. Elemental analysis determined the oxygen



content of the synthesized nanoparticles to be 55.59%. This high oxygen percentage could be attributed to either surface oxidation during formation of the NiO NPs or the presence of polyphenolic groups and other carbon-containing biomolecules in the licorice leaf extract [40].



**Figure 6:** (A) shows the FESEM images of NiO NPs. (B) EDX analysis of NiO NPs.

### 3.1.5. Atomic Force Microscopy (AFM)

The AFM was used to investigate the surface morphology of nanoparticles. The root mean square height (Sq), mean particle size distribution, and surface roughness (Sa) calculated using SPIP mountains software.

The two and three- dimensional images, represented in Figure (7-A), show that the NiO NPs in the 2D image appear spherical with a uniform distribution in the scanned area (3.58 x 3.58  $\mu$ m) with some aggregation which may be the result of the effect of plant extraction into nanoparticles. The mean diameter of particles of 241nm in the desired area was found to be 53.20 nm as shown in figure (7-B). The samples were scanned using the tapping mode, while the surface roughness was determined by changes in the height and represented by parameters Sa (7.358 nm) and Sq (10.28nm), pointing to their highly rough and irregular surface morphology [31].

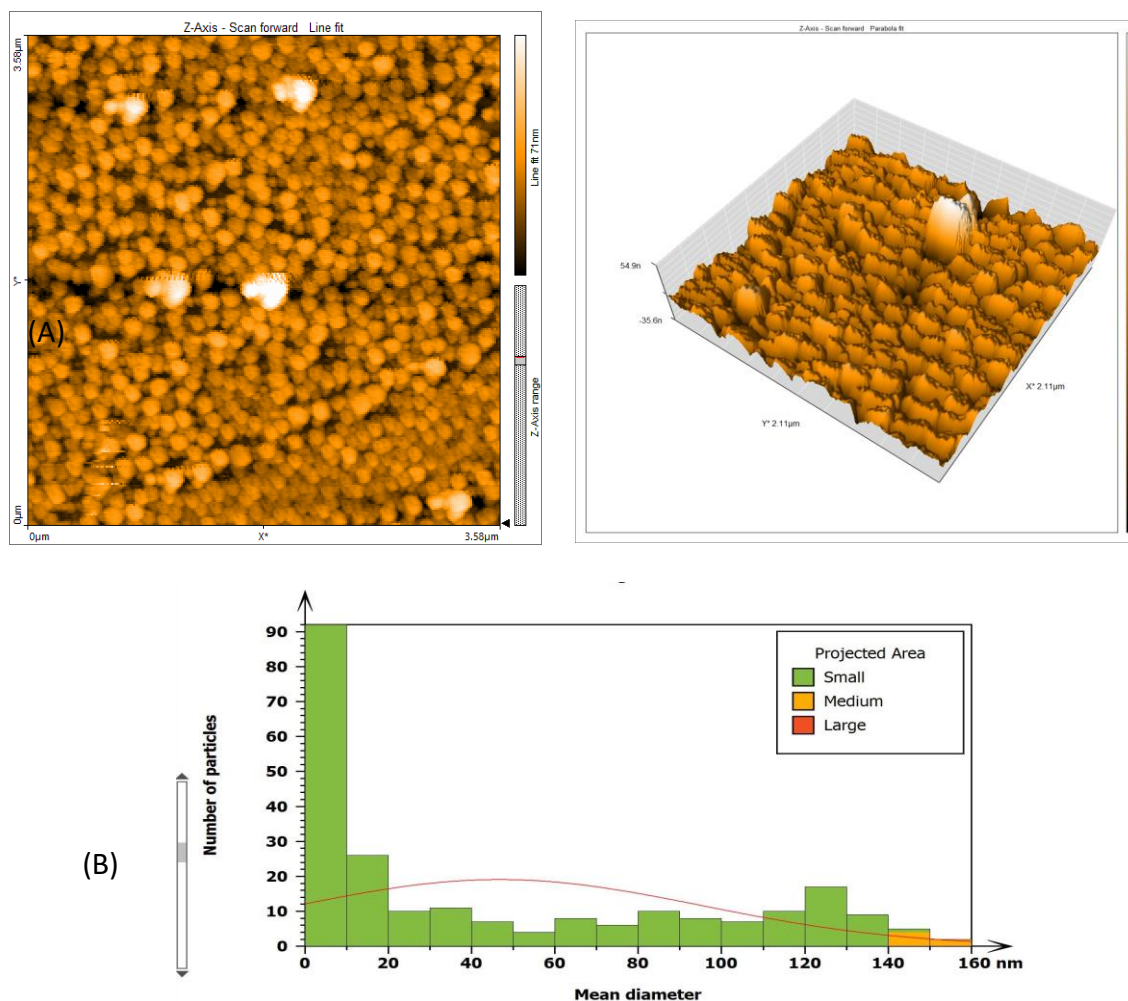


**Figure 7:** (A) shows an AFM pictures of NiO nanoparticles made by green methods. (B) Distribution of diameter ranges of nanoparticles

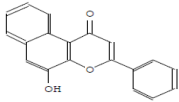
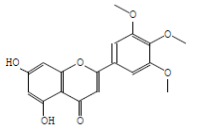
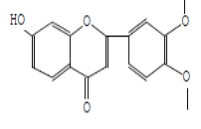
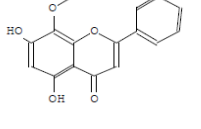
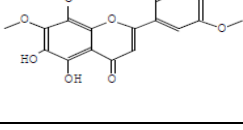
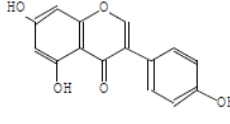
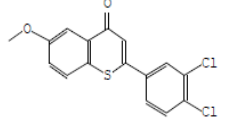
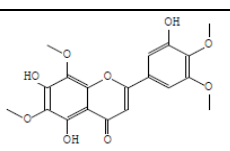
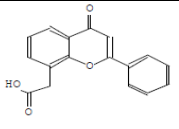
### 3.2. Gas chromatography-mass spectrometry (GC-MS) analysis

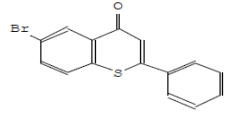
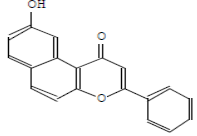
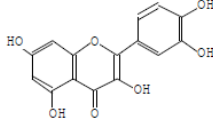
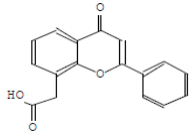
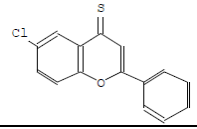
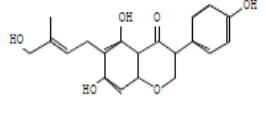
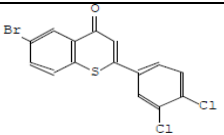
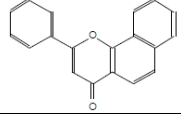
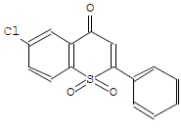
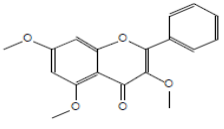
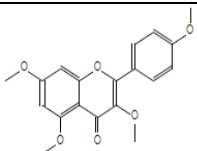
The Inert column is a nonpolar analytical tool constructed from fused-silica capillary. Its inner surface is chemically bonded with dimethylpolysiloxane. This column is designed for direct interfacing with a Mass Spectrometer. For the gas chromatography analysis, helium was used as the carrier gas flowing through the 30-meter-long column at a rate of 30 ml/min. The injector port temperature was set to 250°C to volatilize the sample for subsequent separation and detection. The oven temperature program was as follows: the initial holding temperature was 30°C for 3 minutes, followed by an increase to 200°C at a rate of 3°C/min, and a final isothermal hold at 200°C for 15 minutes. A 2 µL volume of a 0.2% liquid sample solution diluted in ethanol was injected at 280°C. The split ratio for the inlet was set to 2:1. The ionization voltage was 72 electron volts. The ion source temperature is 280 degrees Celsius. The proportional amount of each component was determined by comparing its average area to the total peak areas. The MS was operated using the software provided by the manufacturer. This mass spectroscopy solution software was utilized to control the instrumentation and acquire the spectral data [41].

Phytochemicals are primarily identified by assessing their retention time, molecular formula, molecular weight and peak area. Table 2 lists the 23 substances identified via GC analysis of the ethanolic extract of licorice leaves. Many of these phytochemicals have properties that help explain their role in the biosynthesis of NiO nanoparticles. Specifically, several can act

as reducing agents, transforming  $\text{Ni}^{2+}$  ions to elemental  $\text{Ni}^0$ . Additionally, many are capable of acting as capping ligands, enhancing the colloidal stability of the formed NiO NPs. The presence of these biomolecules likely contributed to increased efficacy of the biosynthesized NiO NPs in biological applications [42].

**Table 2:** GC-MS spectral analysis of ethanolic extract of *Licorice leaves*

No.	Retention time (min)	Name of the compound	Molecular formula	Molecular weight	Peak Area %	Chemical structures
1	3.69	10-Hydroxybenzo[f]flavone	$\text{C}_{19}\text{H}_{12}\text{O}_3$	288	1.9	
2	4.845	4H-1-Benzopyran-4-one, 5,7-dihydroxy-2-(3,4,5-trimethoxyphenyl)-	$\text{C}_{18}\text{H}_{16}\text{O}_7$	344	3.75	
3	5.48	4H-1-Benzopyran-4-one, 2-(3,4-dimethoxyphenyl)-7-hydroxy	$\text{C}_{17}\text{H}_{14}\text{O}_5$	298	1.91	
4	6.7	Flavone, 5,7-dihydroxy-8-methoxy	$\text{C}_{16}\text{H}_{12}\text{O}_5$	284	1.96	
5	6.772	4H-1-Benzopyran-4-one, 2-(3,4-dimethoxyphenyl)-5,6-dihydroxy-7,8-dimethoxy-	$\text{C}_{19}\text{H}_{18}\text{O}_8$	374	2.58	
6	6.985	4',5,7-Trihydroxyisoflavone	$\text{C}_{15}\text{H}_{10}\text{O}_5$	270	4.19	
7	7.76	3',4'-Dichloro-6-methoxythioflavone	$\text{C}_{16}\text{H}_{10}\text{Cl}_2\text{O}_2\text{S}$	336	2.00	
8	8.44	4H-1-Benzopyran-4-one, 5,7-dihydroxy-2-(3-hydroxy-4,5-dimethoxyphenyl)-6,8-dimethoxy-	$\text{C}_{19}\text{H}_{18}\text{O}_9$	390	3.23	
9	8.957	Flavone acetic acid	$\text{C}_{17}\text{H}_{12}\text{O}_4$	280	3.31	

10	9.185	6-Bromothioflavone	C <sub>15</sub> H <sub>9</sub> BrOS	316	2.31	
11	9.441	6-Hydroxybenzo[f]flavone	C <sub>19</sub> H <sub>12</sub> O <sub>3</sub>	288	2.19	
12	9.62	Quercetin	C <sub>15</sub> H <sub>10</sub> O <sub>7</sub>	302	2.28	
13	10.713	Flavone acetic acid	C <sub>17</sub> H <sub>12</sub> O <sub>4</sub>	280	1.88	
14	11.13	6-Chloro-4-thionoflavone	C <sub>15</sub> H <sub>9</sub> ClOS	272	2.43	
15	11.535	5,7,4'-Trihydroxy-6-[3-(hydroxymethyl)but-2-enyl]isoflavone	C <sub>20</sub> H <sub>18</sub> O <sub>6</sub>	354	2.34	
16	11.89	6-Bromo-3',4'-dichlorothioflavone	C <sub>15</sub> H <sub>7</sub> BrCl <sub>2</sub> OS	384	1.89	
17	12.695	4H-Naphtho[1,2-b]pyran-4-one, 2-phenyl-	C <sub>19</sub> H <sub>12</sub> O <sub>2</sub>	272	2.82	
18	12.858	6-Chloro-1-thioflavone-1,1-dioxide	C <sub>15</sub> H <sub>9</sub> ClO <sub>3</sub> S	304	3.55	
19	13.039	4H-1-Benzopyran-4-one, 3,5,7-trimethoxy-2-phenyl-	C <sub>18</sub> H <sub>16</sub> O <sub>5</sub>	312	2.79	
20	13.444	4H-1-Benzopyran-4-one, 3,5,7-trimethoxy-2-(4-methoxyphenyl)	C <sub>19</sub> H <sub>18</sub> O <sub>6</sub>	342	2.45	

21	13.629	2H,6H-Benzo[1,2-b:5,4-b']dipyran-6-one, 7-(2,4-dimethoxyphenyl)-5-methoxy-2,2-dimethyl-	$C_{23}H_{22}O_6$	394	2.09	
22	14.13	5,7,4'-Trihydroxy-6-[3-(hydroxymethyl)but-2-enyl]isoflavone	$C_{20}H_{18}O_6$	354	3.54	
23	14.787	Acacetin	$C_{16}H_{12}O_5$	284	3.18	

### 3.3. Effect of Nickel oxide nanoparticles on the viability of MG-63 Cells

The effect of NiO nanoparticles on osteosarcoma cancer cells was examined by exposing MG-63 cells to various doses (20, 50, 100, 250 and 500  $\mu\text{g/ml}$ ) for 24 h and the viability of the cells was assessed by MTT assay (Fig. 8). It was observed that NiO nanoparticles biosynthesized from Licorice leaves exhibited a dose-dependent inhibitory effect on the proliferation of MG-63 cancer cells, with increasing concentrations leading to enhanced suppression. The inhibitory concentration ( $IC_{50}$  value) was determined to be 149.71  $\mu\text{g/ml}$ . the study found that the presence of a higher concentration of NiO nanoparticles led to decreased survival of cancer cells.

The Cell viability of MG-63 Cells reduced to 28.78% at maximum concentration (500  $\mu\text{g/ml}$ ) compared to 80.79 % for HFF cell viability while the ability of NiO nanoparticles as anticancer potential was reduced with decreased nanoparticles concentration as shown in Figures (9) and (10).

The widely accepted mechanism of cytotoxicity with NiO nanoparticles causes oxidative stress, inflammation and subsequent damage to DNA, proteins, and cell membranes [43]. The physicochemical properties of NPs such as their large surface area to volume ratio of nanoparticles and particle size, contribute to their higher chemical reactivity and the activation of an oxidative enzymatic pathway which leads to an increased formation of reactive oxygen species (ROS) such as superoxide radical anions and hydroxyl radicals which are play a vital role in the cell death [5, 44].



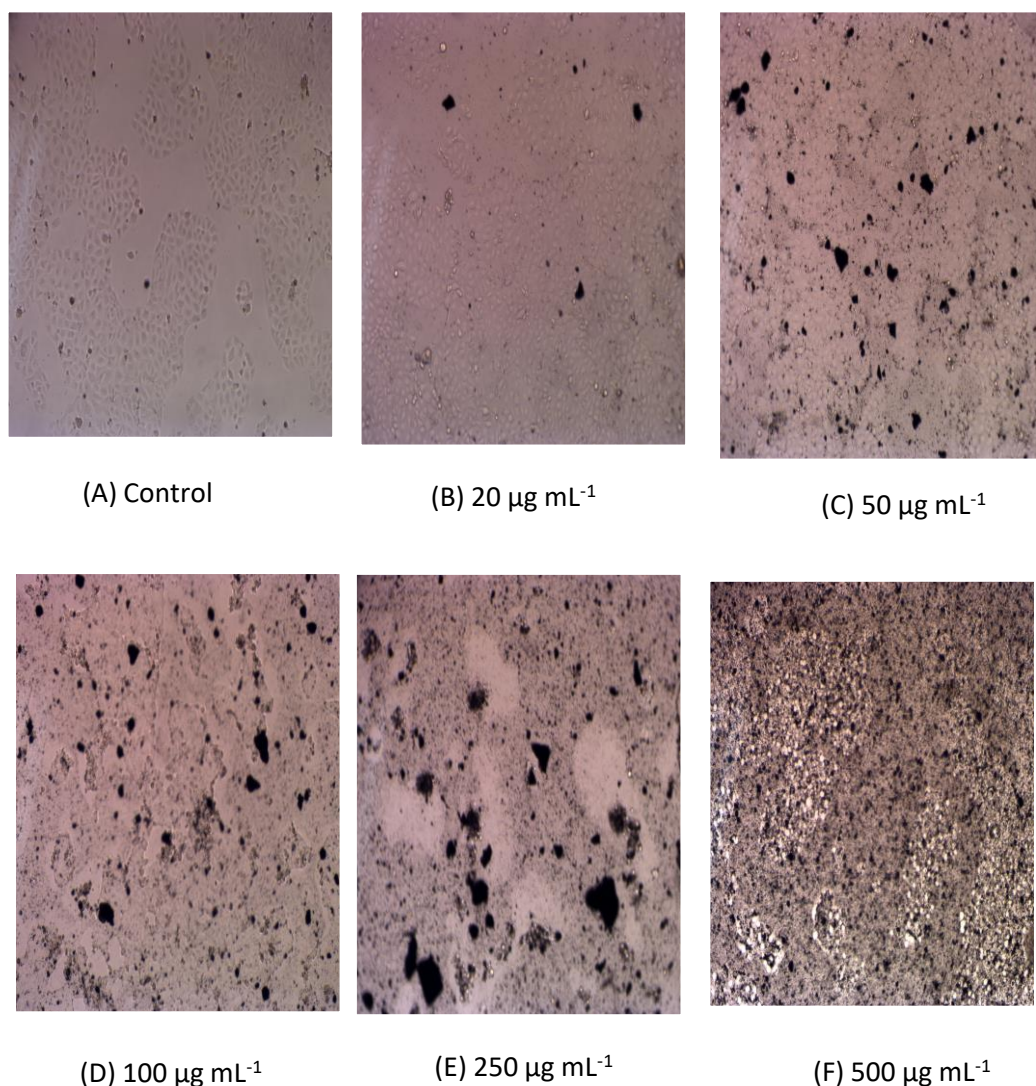


**Figure 8:** Morphological alterations in MG-63 cells treated with NiO NPs (A)Control cells, (B,C,D,E and F) Cells treated with NiO NPs at concentration of 20,50,100,250 and 500  $\mu\text{g/ml}$ . MG-63 cells treated with 500  $\mu\text{g/ml}$  of NiO NPs show a fewer number of viable cells.

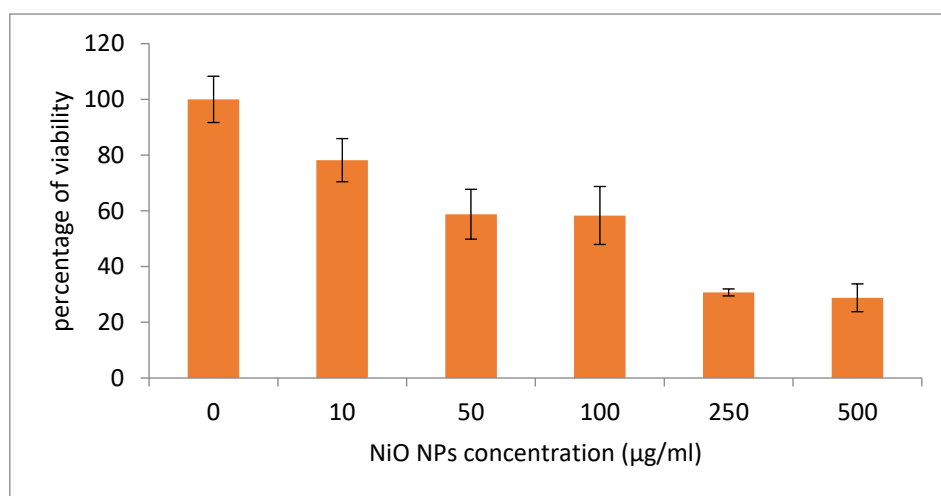


**Figure 9:** MTT assay graph for anticancer activity of green synthesized NiO NPs nanoparticles from *Licorice* leaves

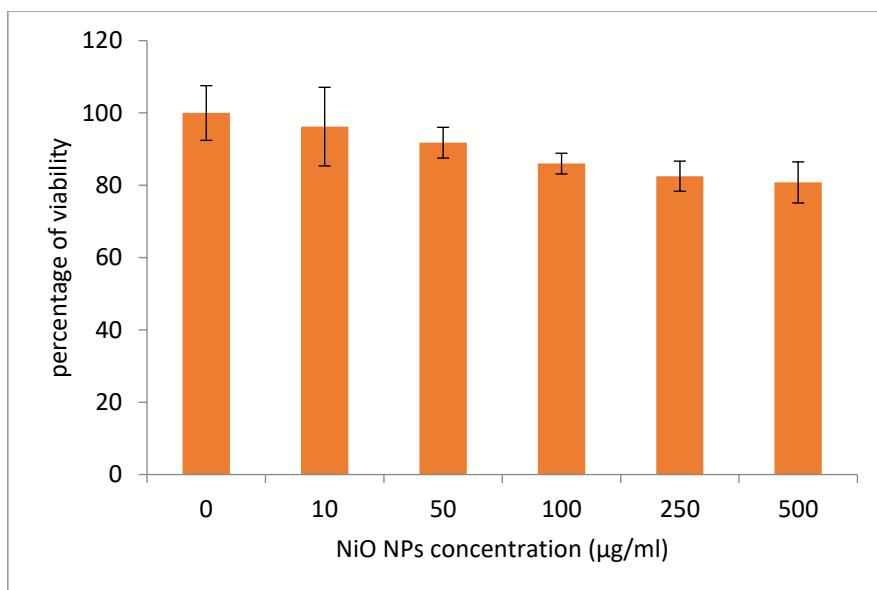


**Figure 10:** MTT assay graph for anticancer activity of HFF cell lines viability

### 3.4. Antibacterial Activity of NiO NPs

Figure 11 illustrates the substantial antibacterial effects of NiO nanoparticles (NPs) against both Gram-negative and Gram-positive bacteria. The Gram-negative bacteria tested were *Escherichia coli* and *Pseudomonas aeruginosa*, while the Gram-positive bacteria were *Staphylococcus aureus* and *Streptococcus* species. The study evaluated various concentrations of NiO NPs, specifically 128, 256, 512, and 1024 μg/ml, demonstrating their efficacy across these different bacterial types. The inhibition zones of recorded diameters (in mm) surrounding the discs 18mm, 18mm, 15mm and 22 mm at higher concentration (1024 μg/ml), respectively while the effectiveness of NiO NPs in low concentration (128 μg/ml) reduced or completely disappears to eliminate microorganisms., as presented in Table (3) and Figure (12).

The proposed mechanisms for the antibacterial activity of NiO NPs involve the generation of Reactive oxygen species (ROS) on the surfaces of nanoparticles such as hydroxyl ions ( $\text{OH}^\cdot$ ), superoxide radicals ( $\text{O}_2^{\cdot-}$ ), and hydrogen peroxide ( $\text{H}_2\text{O}_2$ ). The ROS causes Damage to cellular components such as proteins, DNA and lipids in the cell wall [45-47]. the active phytochemicals compounds found in *Licorice leaves* may contribute to the enhancement the antibacterial activity of the synthesized NiO nanoparticles.

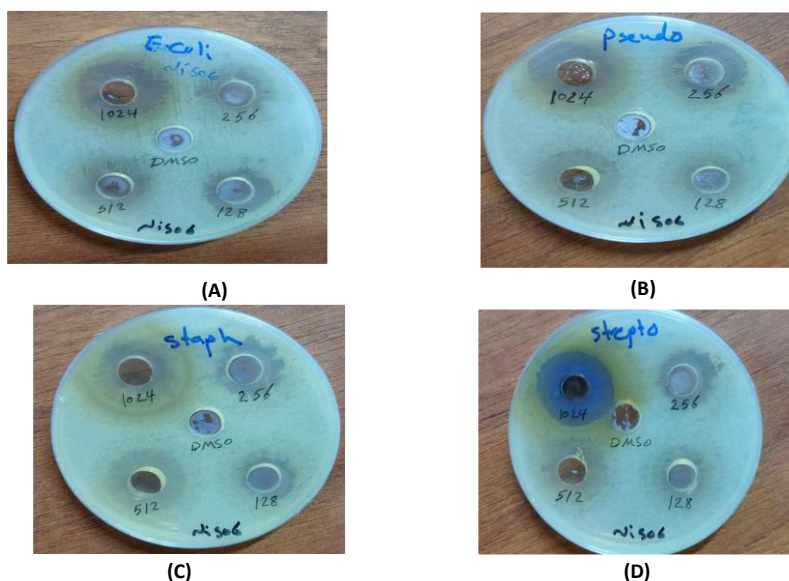


**Figure (11)** Inhibition Zone of **A-** *Escherichia coli* **B-** *Pseudomonas aeruginosa* **C-** *Staphylococci aureus* **D-** *Streptococcus* in response to treatment with the synthesized NiO NPs in different concentration.

**Table 3:** The measured zone of inhibition diameters relating the antimicrobial activity of various concentrations of the biosynthesized NiO NPs against the tested bacterial isolates are recorded.

Concentrations of NiO NPs Bacterial Isolates	1024( $\mu\text{g/mL}$ )	512( $\mu\text{g/mL}$ )	256( $\mu\text{g/mL}$ )	128 ( $\mu\text{g/mL}$ )
<i>Escherichia coli</i>	18	7	7	7
<i>Pseudomonas aeruginosa</i>	18	15	15	Zero
<i>Staphylococci aureus</i>	15	15	12	7
<i>Streptococcus</i>	22	15	8	Zero

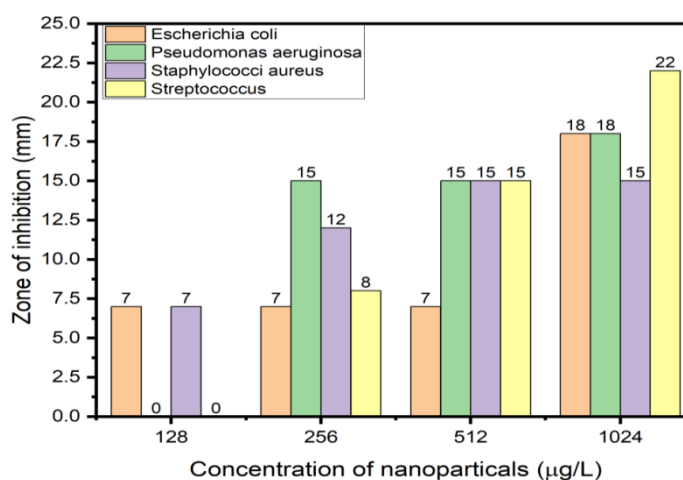


**Figure 12:** The graphics depict the variation in inhibition zone diameters measured at different test concentrations of the NiO nanoparticles

## Conclusion

The synthesized NiO NPs exhibit substantial anticancer on cancer cell line (MG-63) and antibacterial effects on bacterial strains (*Escherichia coli*, *Pseudomonas aeruginosa*, *Staphylococcus aureus* and *Streptococcus*) which are directly proportional to the increase in concentration of NiO NP against Toxicology Evaluation. The study demonstrated that NiO NP was successfully synthesized and characterized using a green method involving Licorice leaves. the flavonoid and other phenolic compounds in plant extract reduce  $Ni^{2+}$  ions into NiO NP which have a promising anticancer and antibacterial activity.

## Acknowledgment

We thank the Chemistry Department, College of Science, University of Baghdad, for supporting our study

## Disclosure and conflict of interest

“Conflict of Interest: The authors declare that they have no conflicts of interest.”

## Authors' Contribution Statement

M.M and W.N. contributed to the design and implementation of the research, to the analysis of the results and to the writing of the manuscript.

## References

- [1] D. Baumhoer, P. Brunner, S. Eppenberger-Castori, J. Smida, M. Nathrath, and G. Jundt, "Osteosarcomas of the jaws differ from their peripheral counterparts and require a distinct treatment approach. Experiences from the DOESAK Registry," *Oral oncology*, vol. 50, no. 2, pp. 147-153, 2014.
- [2] A. Pradhan, K.I.A. Reddy, R.J. Grimer, A. Abudu, R.M. Tillman, S.R. Carter, and L. Jeys, "Osteosarcomas in the upper distal extremities: are their oncological outcomes similar to other sites?," *European Journal of Surgical Oncology (EJSO)*, vol. 41, no. 3, pp. 407-412, 2015.
- [3] C. Gerrand, N. Athanasou, B. Brennan, R. Grimer, I. Judson, and B. Morland., "UK guidelines for the management of bone sarcomas," *Clinical Sarcoma Research*, vol. 6, pp. 1-21, 2016.
- [4] V. D. Seshadri, "Zinc oxide nanoparticles from *Cassia auriculata* flowers showed the potent antimicrobial and in vitro anticancer activity against the osteosarcoma MG-63 cells," *Saudi Journal of Biological Sciences*, vol. 28, no. 7, pp. 4046-4054, 2021.
- [5] J. Chenga, X. Wangb, L.. Qiuc, Y.Lid , N. Marraikie , A.M. Elgorbane and L.Xue., "Green synthesized zinc oxide nanoparticles regulates the apoptotic expression in bone cancer cells MG-63 cells," *Journal of Photochemistry and Photobiology B: Biology*, vol. 202, p. 111644, 2020.
- [6] L. V. Barba-Rosado, D. C. Carrascal-Hernández, D. Insuasty, and C. D. Grande-Tovar, "Graphene Oxide (GO) for the Treatment of Bone Cancer: A Systematic Review and Bibliometric Analysis," *Nanomaterials*, vol. 14, no. 2, p. 186, 2024.
- [7] W. N. J. A. S. Ahmed K. Abass, Abdul Karim M.A. Al-Sammarraie, "Investigation of the electrical, compositional, and magnetic features of hybrid lead oxide nanocomposites," *Eurasian Chemical Communications*, vol. 4, pp. 1044-1053, 2022.
- [8] J. H. Taha, N. K. Abbas, and A. A. Al-Attaqchi, "Synthesis and evaluation of platinum nanoparticles using *F. Carica* fruit extract and their antimicrobial activities," *Baghdad Science Journal*, vol. 20, no 3 .(Suppl.), pp. 1146-1146, 2023.
- [9] S. Majeed, N. F. B. Bakhtiar, M. Danish, M. M. Ibrahim, and R. Hashim, "Green approach for the biosynthesis of silver nanoparticles and its antibacterial and antitumor effect against osteoblast MG-63 and breast MCF-7 cancer cell lines," *Sustainable chemistry and pharmacy*, vol. 12, p. 100138, 2019.
- [10] S. Uddin,J. Iqbal,L. B.Safdar,S. Ahmad,B. A.Abbasi,R. Capasso,M Kazi and U. M. Quraihi., "Green synthesis of BPL-NiONPs using leaf extract of *Berberis pachyacantha*: Characterization and multiple in vitro biological applications," *Molecules*, vol. 27, no. 7, p. 2064, 2022.

- [11] M. F. Altaee, L. A. Yaaqoob, and Z. K. Kamona, "Evaluation of the biological activity of nickel oxide nanoparticles as antibacterial and anticancer agents," *Iraqi Journal of Science*, pp. 2888-2896, 2020.
- [12] A. Amer and L. Karem, "Biological Evaluation and Antioxidant Studies of Nio, Pdo and Pt Nanoparticles Synthesized from a New Schiff Base Complexes. Ibn al-Haitham J Pure Appl Sci. 2022; 35 (4): 170-182," ed.
- [13] D. L. McKay and J. B. Blumberg, "A review of the bioactivity and potential health benefits of chamomile tea (*Matricaria recutita* L.)," *Phytotherapy Research: An International Journal Devoted to Pharmacological and Toxicological Evaluation of Natural Product Derivatives*, vol. 20, no. 7, pp. 519-530, 2006.
- [14] J. B. Zadeh, Z. M. Kor, and M. K. Goftar, "Licorice (*Glycyrrhiza glabra* Linn) as a valuable medicinal plant," *International journal of Advanced Biological and Biomedical Research*, vol. 1, no. 10, pp. 1281-1288, 2013.
- [15] H. Hayashi and H. Sudo, "Economic importance of licorice," *Plant Biotechnology*, vol. 26, no. 1, pp. 101-104, 2009.
- [16] Z. Y. Wang and D. W. Nixon, "Licorice and cancer," *Nutrition and cancer*, vol. 39, no. 1, pp. 1-11, 2001.
- [17] F. S. MOHAMMED, N. KORKMAZ, M. DOĞAN, A. E. ŞABİK, and M. SEVİNDİK, "Some medicinal properties of *Glycyrrhiza glabra* (Licorice)," *Journal of Faculty of Pharmacy of Ankara University*, vol. 45, no. 3, pp. 524-534, 2021.
- [18] G. Pastorino, L. Cornara, S. Soares, F. Rodrigues, and M. B. P. Oliveira, "Liquorice (*Glycyrrhiza glabra*): A phytochemical and pharmacological review," *Phytotherapy research*, vol. 32, no. 12, pp. 2323-2339, 2018.
- [19] A. M. Aly, L. Al-Alousi, and H. A. Salem, "Licorice: a possible anti-inflammatory and anti-ulcer drug," *Aaps Pharmscitech*, vol. 6, pp. E74-E82, 2005.
- [20] H. S. Cheema, O. Prakash, A. Pal, F. Khan, D. U. Bawankule, and M. P. Darokar, "Glabridin induces oxidative stress mediated apoptosis like cell death of malaria parasite *Plasmodium falciparum*," *Parasitology international*, vol. 63, no. 2, pp. 349-358, 2014.
- [21] A. S. Chakotiya, A. Tanwar, A. Narula, and R. K. Sharma, "Alternative to antibiotics against *Pseudomonas aeruginosa*: Effects of *Glycyrrhiza glabra* on membrane permeability and inhibition of efflux activity and biofilm formation in *Pseudomonas aeruginosa* and its in vitro time-kill activity," *Microbial pathogenesis*, vol. 98, pp. 98-105, 2016.
- [22] T. Fukai, A. Marumo, K. Kaitou, T. Kanda, S. Terada, and T. Nomura, "Antimicrobial activity of licorice flavonoids against methicillin-resistant *Staphylococcus aureus*," *Fitoterapia*, vol. 73, no. 6, pp. 536-539, 2002.
- [23] J. Cinatl, B. Morgenstern, G. Bauer, P. Chandra, H. Rabenau, and H. Doerr, "Glycyrrhizin, an active component of liquorice roots, and replication of SARS-associated coronavirus," *The Lancet*, vol. 361, no. 9374, pp. 2045-2046, 2003.
- [24] A. V. Lohar, A. M. Wankhade, M. Faisal, and A. Jagtap, "Review on *Glycyrrhiza glabra* Linn (liquorice)—An excellent medicinal plant," *European Journal of Biomedical*, vol. 7, no. 7, pp. 330-334, 2020.
- [25] L. Siracusa, A. Saija, M. Cristani, F. Cimino, M. D. Arrigo, D. Trombetta, F. Rao, and G. Ruberto, "Phytocomplexes from liquorice (*Glycyrrhiza glabra* L.) leaves—Chemical characterization and evaluation of their antioxidant, anti-genotoxic and anti-inflammatory activity," *Fitoterapia*, vol. 82, no. 4, pp. 556-546, 2011.
- [26] L. Frattaruolo, G. Carullo, M. Brindisi, S. Mazzotta, L. Bellissimo, V. Rago, R. Curcio, V. Dolce, F. Aiello, and A. R. Cappello, "Antioxidant and anti-inflammatory activities of flavanones from *Glycyrrhiza glabra* L. (licorice) leaf phytocomplexes: Identification of licoflavanone as a modulator of NF- $\kappa$ B/MAPK pathway," *Antioxidants*, vol. 8, no. 6, p. 186, 2019.
- [27] O. Chouitah, B. Meddah, A. Aoues, and P. Sonnet, "Chemical composition and antimicrobial activities of the essential oil from *Glycyrrhiza glabra* leaves," *Journal of Essential Oil Bearing Plants*, vol. 14, no. 3, pp. 284-288, 2011.
- [28] J. D. M. Biondi, C. Rocco, and G. Ruberto, "New Dihydrostilbene Derivatives from the Leaves of *Glycyrrhiza glabra* and Evaluation of their Antioxidant Activity," *Journal of natural products*, vol. 66, no. 4, pp. 477-480, 2003.



- [29] Y.dong, M.Zhao, D. Sun Waterhouse, M.Zhuang, H. Chen, M. Feng and L.Lin., "Absorption and desorption behaviour of the flavonoids from Glycyrrhiza glabra L. leaf on macroporous adsorption resins," *Food chemistry*, vol. 168, pp. 538-545, 2015.
- [30] G. Dastagir and M. A. Rizvi, "Glycyrrhiza glabra L.(Liquorice)," *Pakistan journal of pharmaceutical sciences*, vol. 29, no. 5, 2016.
- [31] N. Jawad and K. Hassan, "Structural Characterization of NiO Nanoparticles Prepared by Green Chemistry Synthesis Using Arundo donax Leaves Extract," in *Journal of Physics: Conference Series*, 2021, vol. 181, no. 1, p. 012007: IOP Publishing.
- [32] B. H. Shnawa, P. J. Jalil, S. M. Hamad, and M. H. Ahmed, "Antioxidant, protoscolicidal, hemocompatibility, and antibacterial activity of nickel oxide nanoparticles synthesized by Ziziphus spina-christi," *Bionanoscience*, vol. 12, no. 4, pp. 1264-1278, 2022.
- [33] H. Balto, M. Amina, R. S. Bhat, H. M. Al-Yousef, S. H. Auda, and A. Elansary, "Green Synthesis of Nickel Nanoparticles Using Salvadora persica and Their Application in Antimicrobial Activity against Oral Microbes," *Microbiology Research*, vol. 14, no. 4, pp. 1879-1893, 2023.
- [34] A. A. Ezhilarasi, J. J. Vijaya, K. Kaviyarasu, M. Maaza, A. Ayeshamariam, and L. J. Kennedy, "Green synthesis of NiO nanoparticles using Moringa oleifera extract and their biomedical applications: Cytotoxicity effect of nanoparticles against HT-29 cancer cells," *Journal of Photochemistry and Photobiology B: Biology*, vol. 164, pp. 352-360, 2016.
- [35] Z. Sabouri, A. Akbari, H. A. Hosseini, A. Hashemzadeh, and M. Darroudi, "Eco-friendly biosynthesis of nickel oxide nanoparticles mediated by okra plant extract and investigation of their photocatalytic, magnetic, cytotoxicity, and antibacterial properties," *Journal of Cluster Science*, vol. 30, pp. 1425-1434, 2019.
- [36] I. M. Ibrahim, A. S. Mohammed, and A. Ramizy, "Energy Band Diagram of NiO: Lu<sub>2</sub>O<sub>3</sub>/n-Si heterojunction," *Iraqi Journal of Science*, vol. 59, no. 1B, pp. 287-293, 2018.
- [37] Z. N. Abdul-Ameer, "Novel Co-Precipitation method for synthesis of Nanostructured Nickel Oxide in accordance to PH: Structural and Optical Properties as an Active optical filter," *Ibn Al-Haitham Journal For Pure and Applied Science*, vol. 32, no. 1, pp. 1-6, 2019.
- [38] M. Hafeez, R. Shaheen, B. Akram, M. N. Ahmed, Z. ul-Abdin, S. Haq, S. Ud Din, M. Zeb and M. A. Khan., "Green synthesis of nickel oxide nanoparticles using Populus ciliata leaves extract and their potential antibacterial applications," *South African Journal of Chemistry*, vol. 75, pp. 168-173, 2021.
- [39] A. A. Ezhilarasi, J. J. Vijaya, K. Kaviyarasu, L. J. Kennedy, R. J. Ramalingam, and H. A. Al-Lohedan, "Green synthesis of NiO nanoparticles using Aegle marmelos leaf extract for the evaluation of in-vitro cytotoxicity, antibacterial and photocatalytic properties," *Journal of Photochemistry and Photobiology B: Biology*, vol. 180, pp. 39-50, 2018.
- [40] H. Gebretinsae, M. Tsegay, and Z. Nuru, "Biosynthesis of nickel oxide (NiO) nanoparticles from cactus plant extract," *Materials Today: Proceedings*, vol. 36, pp. 566-570, 2021.
- [41] M. R. Meyer, "Hans-Joachim Hübschmann: Handbook of GC-MS: fundamentals and applications," ed :Springer, 2016.
- [42] T. Zahra, K. S. Ahmad, and S. Sharif, "Identification and implication of organic compounds of Viola odorata: a potential source for bio-fabrication of nickel oxide nanoparticles," *Applied Nanoscience*, vol. 11, pp. 1593-1603, 2021.
- [43] M. A. J. Kouhbanani, Y. Sadeghipour, M. Sarani, E. Sefidgar, S. Ilkhani, A. M. Amani and N. Beheshtkhoo., "The inhibitory role of synthesized Nickel oxide nanoparticles against Hep-G2, MCF-7, and HT-29 cell lines: the inhibitory role of NiO NPs against Hep-G2, MCF-7, and HT-29 cell lines," *Green Chemistry Letters and Reviews*, vol. 14, no. 3, pp. 444-454, 2021.
- [44] C. Egbuna, V. K. Parmar, J. Jeevanandam, S. M. Ezzat, K.C. Patrick, C. O. Adetunji, Johra .Khan, E. N. Onyeike, C. Z. Uche, M. Akram, M. S. Ibrahim, N.M. El Mahdy, C. G. Awuchi, K. Saravanan, H. Tijjani, U. E. Odoh, M. Messaoudi, J. C. Ifemeje, M.C. Olisah, N.J. Ezeofor, and C. G. Ibeabuchi., "Toxicity of nanoparticles in biomedical application: nanotoxicology," *Journal of Toxicology*, vol. 2021, pp. 1-21, 2021.
- [45] L. Yaaqoob, R. Younis, Z. Kamona, M. Altaee, and R. Abed, "Biosynthesis of Nio Nanoparticles Using Prodigiosin Pigment and its Evaluate of Antibacterial Activity Against Biofilm Producing MDR-Pseudomonas Aeruginosa," *Iraqi Journal of Science*, pp. 1171-1179, 2023.

- [46] L. Al-Obidi and T. Al-Noor, "Synthesis, Spectral and Bacterial Studies of Mixed Ligand Complexes of Schiff Base Derived from Methyldopa and Anthranilic Acid with Some Metal Ions," *Ibn AL-Haitham Journal For Pure and Applied Science*, pp. 235-247, 2018.
- [47] G. M. Saleh and S. S. Najim, "Antibacterial activity of silver nanoparticles synthesized from plant latex," *Iraqi Journal of Science*, pp. 1579-1588, 2020.